



**CHALMERS**  
UNIVERSITY OF TECHNOLOGY

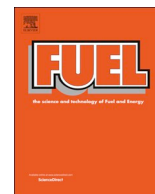
## **Shedding light on the governing mechanisms for insufficient CO and H<sub>2</sub> burnout in the presence of potassium, chlorine and sulfur**

Downloaded from: <https://research.chalmers.se>, 2024-03-13 09:03 UTC

Citation for the original published paper (version of record):

Berdugo Vilches, T., Weng, W., Glarborg, P. et al (2020). Shedding light on the governing mechanisms for insufficient CO and H<sub>2</sub> burnout in the presence of potassium, chlorine and sulfur. Fuel, 273. <http://dx.doi.org/10.1016/j.fuel.2020.117762>

N.B. When citing this work, cite the original published paper.



## Full Length Article

# Shedding light on the governing mechanisms for insufficient CO and H<sub>2</sub> burnout in the presence of potassium, chlorine and sulfur

Teresa Berdugo Vilches<sup>a,\*</sup>, Wubin Weng<sup>b</sup>, Peter Glarborg<sup>c</sup>, Zhongshan Li<sup>b</sup>, Henrik Thunman<sup>a</sup>, Martin Seemann<sup>a</sup>

<sup>a</sup> Division of Energy Technology, Chalmers Tekniska Högskola, Sweden

<sup>b</sup> Division of Combustion Physics, Lund University, P.O. Box 118, S-221 00 Lund, Sweden

<sup>c</sup> Chemical Engineering, Technical University of Denmark, DK-2800 Kgs., Lyngby, Denmark



## ARTICLE INFO

## Keywords:

CO oxidation

Potassium

Inhibition

Combustion

UV absorption spectroscopy

TDLAS

## ABSTRACT

Based on the experiences of insufficient burnout in industrial fluidized bed furnaces despite adequate mixing and availability of oxidizer, the influence of potassium on CO and H<sub>2</sub> oxidation in combustion environments was investigated. The combustion environments were provided by a laminar flame burner in a range relevant to industrial furnaces, i.e. 845 °C to 1275 °C and excess air ratios ranging from 1.05 to 1.65. Potassium, in the form of KOH, was homogeneously introduced into the hot gas environments to investigate its effect on the radical pool. To quantitatively determine key species that are involved in the oxidation mechanism (CO, H<sub>2</sub>, KOH, OH radicals, K atoms), a combination of measurement systems was applied: micro-gas chromatography, broadband UV absorption spectroscopy and tunable diode laser absorption spectroscopy. The inhibition effect of potassium on CO and H<sub>2</sub> oxidation in excess air was experimentally confirmed and attributed to the chain-terminating reaction between KOH, K atoms and OH radicals, which enhanced the OH radical consumption. The addition of chlorine or sulfur could reduce the concentrations of KOH and K atoms and consequently eliminated the inhibition on CO and H<sub>2</sub> oxidation. Existing kinetic mechanisms underestimate the inhibiting effect of potassium and they fail to predict the effect of temperature on CO and H<sub>2</sub> concentration when potassium and sulfur co-exist. This work advances the need to revise existing kinetic mechanisms to fully capture the interplay of K and S in the oxidation of CO and H<sub>2</sub> in industrial fluidized bed furnaces.

## 1. Introduction

Combustion technologies are important sources of heat and electricity in today's society, and they are likely to play a role in the future energy system as a stabilizing complement to intermittent energy sources. To ensure that combustion takes place in the most efficient and clean way, combustion units are subject of strict regulations on emissions, e.g. limits on CO, NO<sub>x</sub>, SO<sub>x</sub>, dioxins. Among the regulated emissions, CO should be kept below 150–500 ppm at the stack for a given excess air concentration of usually 6% for biomass and 11% for waste. The exact values depend on the permissions for different plants and are defined in national and local legislation, e.g. Regulation (20013:253) for combustion of waste in Sweden [1].

A common reason for CO emissions is a local deficit of O<sub>2</sub> due to mixing limitations between fuel and air. Therefore, commercial combustors operate with excess air, resulting in a concentration of some percent O<sub>2</sub> at the stack. The problem of CO emissions is exacerbated in

facilities that combust biomass and inhomogeneous solid fuels such as waste streams. In those cases, moderate temperatures (typically 750–900 °C) are applied to reduce the risk of uncontrolled ash melt and corrosion issues derived from the impurities in the fuel, as well as prevent overheating of the furnace material; a measure that can also challenge the complete oxidation of CO into CO<sub>2</sub>. Besides mixing and temperature, CO oxidation can be influenced by the chemical interaction between the inorganic impurities in the fuel and the fuel oxidation reactions. In fact, even trace levels of active species like alkali compounds can drastically influence the combustion chemistry in thermal conversion processes [2].

The literature on the effect of alkali on the oxidation of CO is inconclusive and the underlying mechanisms are still under discussion. Both, promoting and inhibiting effects of alkali species on CO oxidation have been observed and are theoretically possible [2]. This reflects the strong dependence of the reactions on operating conditions, as well as the complex interrelation between inorganic and organic chemistry.

\* Corresponding author.

E-mail address: [berdugo@chalmers.se](mailto:berdugo@chalmers.se) (T. Berdugo Vilches).

<https://doi.org/10.1016/j.fuel.2020.117762>

Received 30 January 2020; Accepted 31 March 2020

Available online 09 April 2020

0016-2361/ © 2020 The Author(s). Published by Elsevier Ltd. This is an open access article under the CC BY license (<http://creativecommons.org/licenses/by/4.0/>).

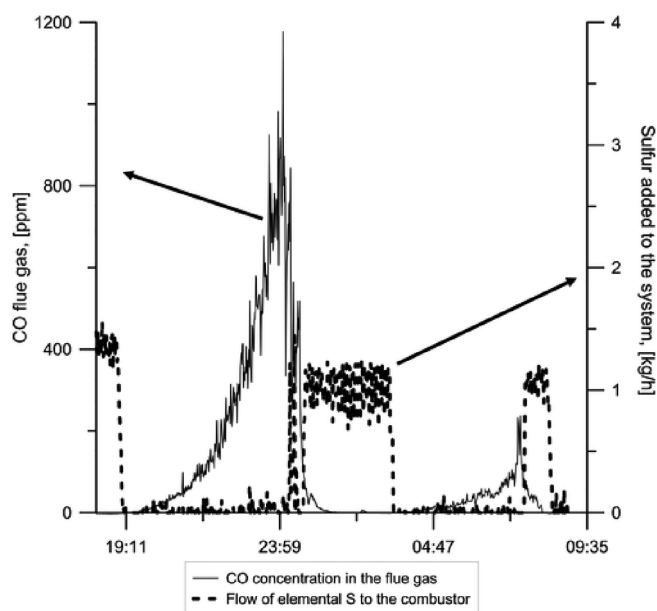
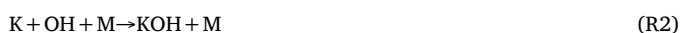


Fig. 1. Influence of accumulation of K in the bed material on the CO emissions from the 12-MW Chalmers circulating fluid bed boiler, and effect of elemental S in mitigating the CO emissions. Combustion of woody biomass at 850 °C with excess air, i.e. 3.5%vol O<sub>2</sub> at the stack. Bed material: Olivine [3].

Previous work in the 12-MW Chalmers circulating fluidized bed (CFB) boiler [3,4] has evidenced the strong inhibiting effect of K on CO oxidation during combustion of biomass in a bed of olivine. Potassium was introduced in the combustor as part of the fuel ash and it accumulated in the bed material, wherefrom it could be released in gas-phase to the reaction environment [4]. Fig. 1 shows the increasing levels of CO over time, as the ash elements accumulate in the olivine bed. Despite the temperature (850 °C) and oxygen concentrations (3.5% vol) were theoretically sufficient to ensure a complete oxidation of the fuel, CO concentrations steadily increased reaching values above 1000 ppm at the stack [3]. The causality between the CO emissions and the presence of K was further confirmed by adding small batches of K salts to the fluidized bed (not shown in the figure). Similar inhibitory effect of CO by Na salts have been observed in smaller units, e.g. in a laboratory-size fluidized bed reactor by Bulewiz et al. [5], and in a 300-kW down-fired radiant furnace by Lissianski et al. [6]. Hindiyarti et al. [7] found that the inhibiting effect of K is also relevant to the oxidation of CO by water vapour in the absence of oxygen in the temperature range 500–1100 °C. The inhibiting effect was proportional to the concentration of potassium and it levelled off at high concentrations (above 500 ppm under the investigated conditions). Contrarily, Ekval et al. [8] did not observe an influence of K on the oxidation of CO during air-combustion of propane in a 100-kW experimental rig at temperatures above 1000 °C, while a promoting effect was found under oxy-fuel conditions.

The inhibiting effect of alkali is mostly attributed to gas-phase radicals removal reactions [2,9,10]. According to Glarborg [2], the main radical removing reactions are R1 and R2. The sequence corresponds to the overall step  $H + OH \rightarrow H_2O$ , where two radicals are removed.



Other trace species than alkali, e.g. sulfur and chlorine, are also known to influence the CO oxidation [2]. The experience of the Chalmers fluidized bed boiler shown in Fig. 1 exemplifies the strong response of the CO emissions to the addition of elemental sulfur. With

1 kg/h of sulfur the CO emissions went rapidly from 1200 ppm to zero, in a system containing 3 tons of olivine bed and fed with 1.8 ton/h of biomass. A similar drastic response was observed in a 26-kW bench-scale diffusion flame during combustion of natural gas under slight sub-stoichiometric conditions and with the addition of 0–100 ppm of SO<sub>2</sub> [11]. In contrast, other work has reported that the addition of SO<sub>2</sub> or higher levels of sulfur in the fuel inhibit CO oxidation, in a laboratory flow reactor [12] and in the fluidized bed reactors [13,14], respectively. Alzueta et al. [15] describe that sulfur promotes the oxidation of CO under nearly stoichiometric conditions, while it mildly inhibits it under fuel lean and rich conditions. Yet, this explanation disagrees with the observations at the Chalmers boiler, where the promoting effect of S on CO oxidation occurred with excess air (3.5% vol in the flue gases or excess air ratio 1.2).

Most previous research indicates that the sulfur chemistry has a direct influence on CO oxidation [11,15], while the experience at Chalmers with K-containing biomass and addition of S [3] also points at interrelations between the S and K chemistry that affect the CO oxidation. Hypothetically, this can occur via e.g. sulfation reactions [8,16] that alter the speciation of K in the reaction environment. Similarly, other species present in biomass such as chlorine could also interfere with the K chemistry [12] and, thereby, influence the CO oxidation. Chlorine by itself have been found to inhibit CO oxidation in a number of investigations. Under moist conditions, Roesler et al. [17] found that trace levels of HCl (0–200 ppm) at atmospheric pressure clearly inhibited CO oxidation in the temperature range of 500–900 °C. Wu et al. [18] found that the inhibiting effect was more pronounced in oxygen-rich conditions than at stoichiometric or oxygen-lean conditions. The inhibiting effect of chlorine has also been observed under fluidized bed operation in the CANMET 0.8 MW CFB combustor using coal as fuel and operating at 850 °C [19,20].

Biomass and waste fuels typically contain chlorine, sulfur and potassium. An understanding of the CO oxidation in large scale combustors calls for a better knowledge of the interplay of these species on the oxidation chemistry. The aim of this work is to shed light on the governing mechanisms for insufficient CO burnout due to the presence of K, despite adequate mixing and availability of oxidizer that has been observed in large scale combustors. A laminar burner system was employed to map the influence of K in the oxidation of CO covering reaction conditions relevant to combustion of biomass and solid waste in fluidized bed combustors, i.e., mild temperature, excess air and co-existence of trace elements. CO oxidation was investigated in the presence of K, S and Cl. The work involves a quantitative study in combustion environments with well-controlled temperature and oxidation conditions, with quantitative measurement of KOH, K-atom, OH radical, CO and H<sub>2</sub>. The suitability of existing kinetic mechanisms to explain the results was assessed and discussed.

## 2. Experimental

Experiments were carried out with a CH<sub>4</sub>/N<sub>2</sub>/O<sub>2</sub> flame generated in a multi-jet burner and the flue gas composition was analysed under various flame conditions, notably temperature and excess air ( $\lambda$ ). The conditions investigated are summarized in Table 1, where the excess air ratio ranges from 1.04 to 1.67 and the temperature ranges from 1275 to 845 °C. The range was chosen to cover  $\lambda = 1.2$  and temperature of 845 °C, as they correspond to the flue gas conditions typically found in commercial fluidized bed combustors, as well as those applied in the Chalmers system when the effect of K and S has been evidenced.

Seeding of K-, S- and Cl-containing species were conducted under the flame conditions described in Table 1 to investigate their effect on the oxidation of CO. Further details on the seeding system are described in subsection 2.2. Two sets of experiments were defined to systematically address two questions: (1) the influence of potassium on the oxidation of CO at different flame conditions; and (2) the influence of sulfur and chlorine, respectively, on the oxidation of CO in co-existence

**Table 1**  
Flame conditions investigated.

Flame Case	Gas flow rate (sl/min)					Excess air ratio $\lambda$	Gas product Temperature $T$ (°C)
	Jet-flow			Co-flow			
	CH <sub>4</sub>	Air	O <sub>2</sub>	N <sub>2</sub>	Air		
T1O1	2.69	13.29	2.80	30.30	0.00	1.04	1275
T2O1	2.48	12.91	2.45	35.35	0.00	1.04	1115
T3O1	2.27	11.84	2.25	40.40	0.00	1.04	985
T4O1	1.86	9.68	1.83	40.40	0.00	1.04	845
T4O2	1.86	9.68	1.83	35.35	5.04	1.32	845
T4O3	1.86	9.68	1.83	29.24	11.13	1.67	845

with potassium. The series of experiments carried out in each set are listed in Table 2. In the first set, potassium was firstly added in different concentrations at constant temperature and excess air ratio (series K1); secondly, the excess air ratio was varied at constant temperature and with a fixed seeding rate of potassium (series K2); and thirdly, the temperature was varied at constant excess air ratio and seeding rate of potassium (series K3). In the second experimental set, the influence of sulfur in co-existence with a fixed seeding flow of potassium was investigated at different temperatures while keeping the excess air ratio constant (series SK). Finally, the effect of chlorine was investigated with a single test (labelled ClK in Table 2) that involved the simultaneous addition of K and Cl, and that was compared to a similar case with addition of K and in the absence of Cl.

The concentrations of CO and H<sub>2</sub> in the flue gas was measured with a micro gas chromatograph ( $\mu$ -GC); the concentration of K atoms by a TDLAS system; and the concentrations of KOH, KCl and OH radicals by UV absorption spectroscopy. The burner, seeding system and the measurement techniques applied are described in detail below.

### 2.1. Burner

The multi-jet burner applied enables the generation of a hot gas environments with an even temperature distribution. The detailed structure of the burner was described by Weng et al. [21], and only a brief description is given here. The burner was comprised of two chambers, namely the jet chamber and the co-flow chamber. The premixed CH<sub>4</sub>/air/O<sub>2</sub> gas mixtures were introduced into the jet chamber and evenly distributed to 181 steel tubes with an inner diameter of 1.6 mm. Premixed flames anchored on the jet tubes to provided hot flue gas, which generated a hot gas environment above the outlet (85 mm  $\times$  47 mm) of the burner for the present study. Each tube was surrounded by even co-flow gases, air/N<sub>2</sub>, which was introduced through the co-flow chamber. All the gas flows were controlled by mass flow controllers (Bronkhorst). The temperature information was obtained through a two-line atomic fluorescence thermometry system of indium atoms as described by Borggren et al. [22].

**Table 2**  
Experimental series according to the question investigated.

Experimental sets	Series	Variable	Range of variation	Flame conditions*	Others
(1) Effect of potassium on CO oxidation	K1	Potassium seeding	0–32 ppm	T4O1	
	K2	Excess air ratio	1.04–1.67	T4O1, T4O2, T4O3	K-seeding 11 ppm
	K3	Temperature	845–1275 °C	T1O1, T2O1, T3O1, T4O1	K-seeding 11 ppm
(2) Effect of Cl and S on CO oxidation in co-existence with K	SK	Temperature	845–1275 °C	T1O1, T2O1, T3O1, T4O1	K-seeding 11 ppm S-seeding 150 ppm
	ClK	–	–	T4O1	K-seeding 11 ppm Cl-seeding 400 ppm

\*Flame conditions described in detail in Table 1.

### 2.2. Seeding of K, S and Cl

To introduce potassium into the hot gases, a water solution of potassium carbonate with a concentration of 0.5 mol/l was used. As shown in Fig. 2, solution fogs were generated through an ultrasonic fogger and transported by air into the jet chamber. As the potassium carbonate passed through the flames, gas-phase potassium hydroxide can be formed in the hot gas. The potassium concentration in the hot gas could be adjusted from 0 to 31 ppm by varying the flow rate of the air for transporting solution fogs. The concentration of total potassium seeded into the hot flue gas was estimated from the measurements of KOH and K atoms. The seeding of trace amount of K<sub>2</sub>CO<sub>3</sub> was observed to have negligible effect on the flue gas temperature.

In the experiments with sulfur, SO<sub>2</sub> was seeded from a gas cylinder into the hot gas after the mixing with co-flow air/N<sub>2</sub>. To seed chlorine to the flame, chloroform (CHCl<sub>3</sub>) was added into the hot gas system. The CHCl<sub>3</sub> liquid was stored in a bubbler and kept at 10 °C using a chilled bath (PolyScience). A N<sub>2</sub> flow was used to carry CHCl<sub>3</sub> vapor into the jet chamber. Potassium chloride was generated by the co-seeding of potassium carbonate. The seeding of sulfur was done at a concentration of 150 ppm while the seeding of chlorine was approximately 400 ppm, which could fully convert KOH in to K<sub>2</sub>SO<sub>4</sub> or KCl at the temperature of 845 °C.

### 2.3. GC system

The micro-gas chromatograph ( $\mu$ -GC) was a Varian CP4900 with two channels equipped with a PoraplotQ and a M S5Å column, and using He and Ar as carrier gases, respectively. A sampling tube made by stainless steel was used to extract the flue gas at a height of about 5 mm above the burner outlet. A gas sample of approximately 300 mL was collected in a gas bag with the help of a syringe. During sampling, the gas was cooled down in the sampling tube, and it was filtered and dried in a LC-NH<sub>2</sub> adsorption column before entering the gas bag. Thereafter, the gas bag was connected to the inlet of the  $\mu$ -GC, so the instrument could take samples from it.

For each test, one gas bag was filled with a sample gas, and its content was analysed five times, i.e. five repeat chromatograms were created per flame conditions. Each chromatogram is the result of a point-injection (10–30 ms sampling time), which was taken in intervals of 4 min to allow the necessary analysis time required by the  $\mu$ -GC. The concentrations of H<sub>2</sub> and CO presented in this work for each test are the average of the five repeat chromatograms, and the error bars represent the corresponding standard deviation.

### 2.4. TDLAS system

The TDLAS system applied in the measurement of K atoms has been previously described in refs. [23,24]. In this system, a laser at wavelength of 769.89 nm was used to detect the potassium atoms with its transition of 4<sup>2</sup>S<sub>1/2</sub>  $\rightarrow$  4<sup>2</sup>P<sub>1/2</sub>. The laser was provided by an external cavity laser (Toptica, DL100), and it had a power of about 3 mW and a beam size of about 1 mm<sup>2</sup>. The cavity laser was controlled by an

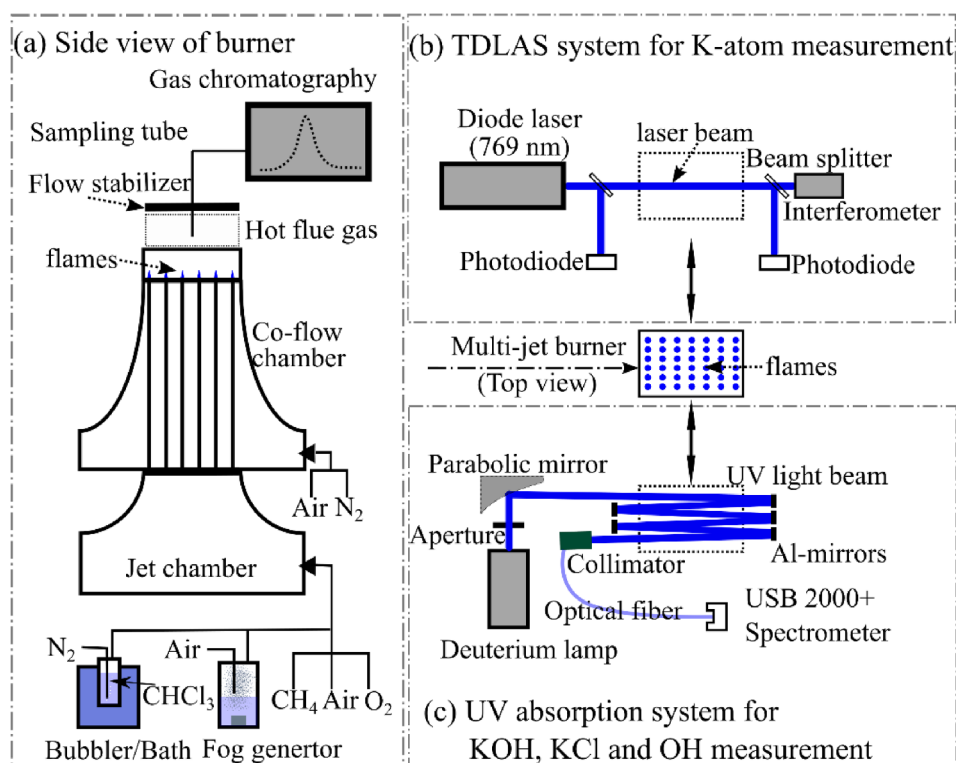


**Fig. 2.** Schematic of the experimental setup. (a) The structure of the burner system with GC sampling system. (b) TDLAS system for K-atom measurement. (c) UV absorption spectroscopy system for quantitative measurements of KOH, KCl and OH radical.

analogy control package with a temperature control module (DTC 110), a current control module (DCC 110), and a scan module (SC 110). The scan module was adopted to make the laser have scanning of the wavelength with a range over 35 GHz at a repetition rate of 100 Hz. The power of the laser was monitored by two photodiodes (PDA100A, Thorlabs), and the scanning range was measured by a high-finesse confocal Fabry-Perot etalon (Topoca, FPI 100), shown in Fig. 2(b). As the laser passed through the hot flue gas containing potassium atoms, the light was absorbed and the concentration of potassium atoms can be derived through the Beer-Lambert law [24,25]. In the present study, the laser beam located at about 5 mm above the burner outlet with a path length of 8.5 cm. The potassium line was determined to have a Voigt profile with a full width at half maximum (FWHM) of 5.34 GHz.

### 2.5. UV absorption spectroscopy system

In the experiments, the concentrations of K atoms, KOH, KCl and OH radicals were measured by UV absorption spectroscopy in the hot gas environments. As shown in Fig. 2(c), a deuterium lamp was used to generate a collimated UV light with a beam size of about 5 mm. The UV light was guided by five UV-enhanced aluminium mirrors to pass through the hot gas with a path length of 522 mm [26]. After the passage, the light was collected and analysed by a spectrometer.

The experimental absorbance data were obtained through the division between the intensity of UV light after the passage of the flame with potassium seeding and the one without potassium seeding. It was used to determine the concentration of KOH and KCl in the hot gas through the Beer-Lambert law. In the calculation, the UV absorption cross-sections of KOH and KCl measured by Weng et al. [24] was used. Typical UV absorption spectrum obtained in KOH concentration measurement are shown in Fig. 3 represented by the black dots. Two absorption peaks centred at around 250 nm and 330 nm can be observed due to the absorption of gas-phase KOH, as described in our previous studies. The absorbance of KOH was simulated using its UV absorption cross-sections, and it could be well overlapped to the measured results

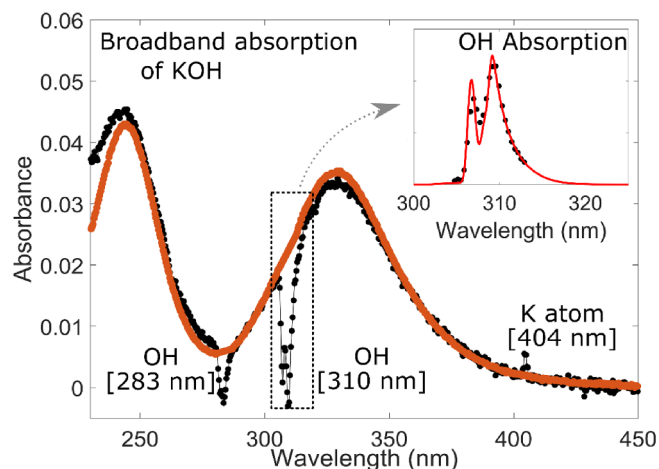


**Fig. 3.** UV absorption spectrum obtained for KOH and OH measurement. The measured absorbance values were presented with black dot and the corresponding fitting curves based on UV-absorption cross-section of KOH [24] and OH [27,28] were shown with red lines. (For interpretation of the references to colour in this figure legend, the reader is referred to the web version of this article.)

as the concentration was set to 11.5 ppm (see Fig. 3 with a red line). The differences between the measured one and the simulated one are the additional absorption at around 404 nm and two dips at around 283 nm and 310 nm. The former one was from the K-atom absorption, while those two dips were formed due to the reduction of OH radicals in the flame after the seeding of potassium. In the measurement of OH radicals, the absorption at around 310 nm were obtained through the division between the intensity of UV light after the passage of the flame and the one without flame. A typical experimental result was shown in the inset of Fig. 3 with black dots. This measured OH absorbance can be fitted (as shown by the solid line) to retrieve the OH concentration

through LIFBASE [28]. As a result of the line-of-sight nature of the absorption spectroscopy technique, the concentration obtained by this method is the average concentration along the horizontal direction from the centre to the edge of the hot flue gas.

### 3. Modelling

The simulations were conducted using Chemkin PRO [29] as described by Weng et al. [30]. A one-dimensional stagnation reactor in Chemkin PRO was adopted to simulate the reaction occurring in the hot flue gas along the central axial direction. The gas inlet of the reactor was assigned to be the mixture of the hot flue gas at 3 mm from the jet flame fronts and the co-flow gas. The composition of the hot flue gas produced from the premixed jet flames was obtained using a one-dimensional free propagation premixed flame model in Chemkin PRO with the GRI-3.0 mechanism [31]. The temperature along the axial direction in the reactor was set to be the one measured by a type B thermocouple in the burner. The measured temperature was corrected based on the heat transfer theory due to heat losses by thermal radiation. The axial distance in the reactor was set to 64 mm, which was the distance between the flame front and the flow stabilizer. The horizontal distribution of the species concentration was obtained using a one-dimensional opposed-flow model in Chemkin PRO as reported by Weng et al. [30]. Through this model, the reaction between the hot flue gas and the ambient air on the edge of the hot flue gas was mimicked. Average concentrations on the horizontal direction were derived from the horizontal distribution of species obtained in the simulations to obtain a result that could be compared to the measurements by absorption spectroscopy. Thus, both the theoretical and experimental concentrations shown in the results section refer to the average on the horizontal direction.

The modelling was conducted with a chemical kinetic model that accounted for both the K-Cl-S interactions, including chlorination and sulfation of potassium, and the impact of the trace species on the O/H radical pool. With a few changes, the K-Cl-S mechanism reported by Weng et al. [16] was chosen for the calculations. This mechanism draws on previous work on alkali metals [32–34] as well as sulfur [35] and chlorine [36] chemistry. In the present work, the alkali subset was revised, with a particular emphasis on the interaction of potassium species with the radical pool. The full mechanism is available as [Supplementary Material](#).

Reactions of potassium species with the radical pool were discussed in previous work [2,7,32]. Few of these steps have been characterized experimentally, and most rate constants have been estimated by analogy with reactions of sodium and lithium. Most of the K/O/H subset is the same as that proposed by Glarborg and Marshall [32]. However, the thermochemistry for  $\text{KO}_2$  and the rate constant for  $\text{K} + \text{O}_2 + \text{M} = \text{KO}_2 + \text{M}$  were drawn from the more recent work of Sorvajärvi et al. [37]. Under oxidizing conditions, the  $\text{KO}_2$  radical may play an important role due to its relatively high thermal stability. Alkali superoxides have been reported to enhance radical removal in premixed flames [38–41] and  $\text{KO}_2$  is believed to participate in the reaction sequences leading to sulfation of KOH [42]. While the  $\text{K} + \text{O}_2 + \text{M}$  reaction is now well established, there are no measurements available for the chain terminating step  $\text{KO}_2 + \text{OH} = \text{KOH} + \text{O}_2$ . In the present work, we have chosen a rate constant for  $\text{KO}_2 + \text{OH}$  of  $10^{14} \text{ cm}^3 \text{ mol}^{-1} \text{ s}^{-1}$ ; this value is possibly an upper limit. Another reaction of interest is the oxidation of CO by  $\text{KO}_2$  to form  $\text{CO}_2 + \text{KO}$ . Perry and Miller [43] set this step to be very fast, with a rate constant of  $10^{14} \text{ cm}^3 \text{ mol}^{-1} \text{ s}^{-1}$ , but their modelling predictions were not sensitive to the value. The Perry and Miller rate constant, which is sufficiently fast to eliminate inhibition of CO oxidation by potassium species under the present conditions, is not supported by any experimental or theoretical work, and we believe that a more realistic value is  $2 \times 10^{12} \text{ cm}^3 \text{ mol}^{-1} \text{ s}^{-1}$ .

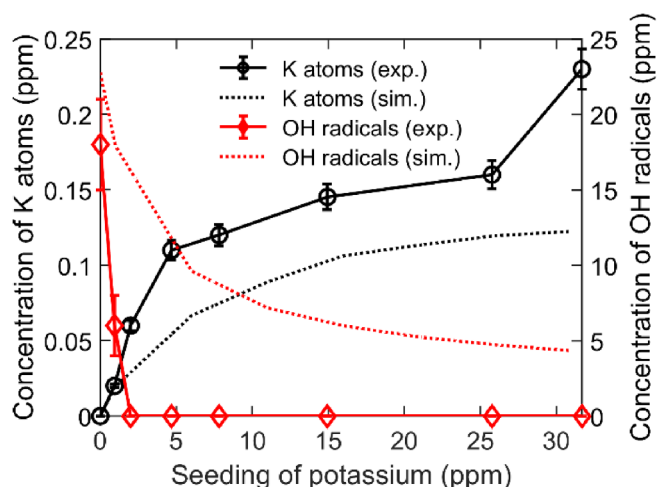


Fig. 4. The variation of the concentration of K atom and OH radical with different amount of potassium seeded into the hot gas at temperature of 845 °C and excess air ratio of 1.04.

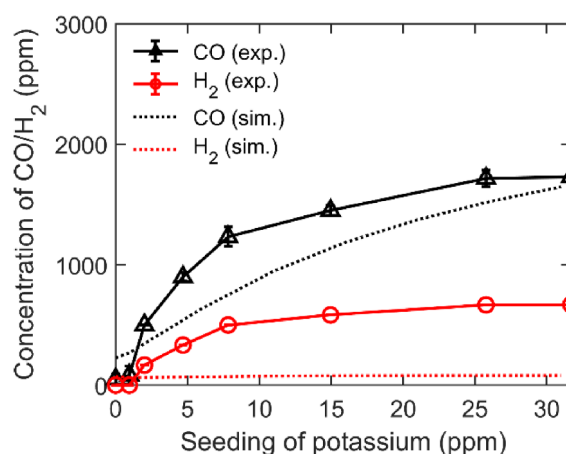


Fig. 5. The variation of the concentration of CO and  $\text{H}_2$  with different amount of total potassium seeded into the hot gas at temperature of 845 °C and excess air ratio of 1.04.

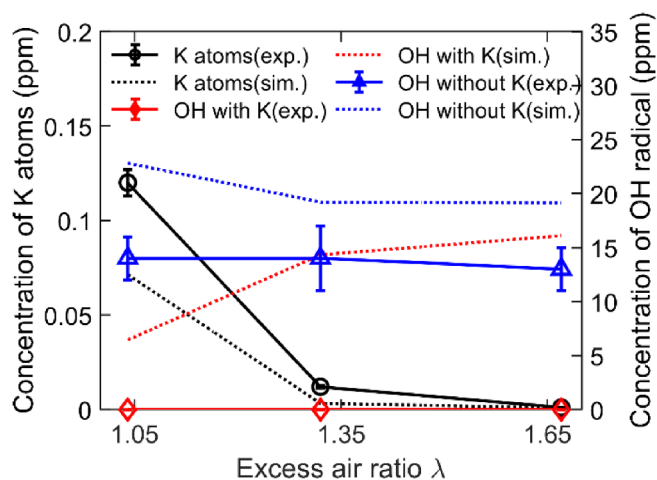


Fig. 6. The variation of the concentration of K atoms and OH radical at different excess air ratio with a temperature of 845 °C and 11 ppm K seeding.

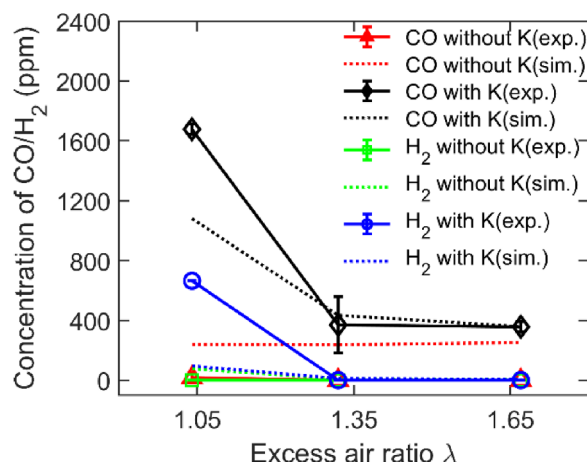


Fig. 7. The variation of the concentration of CO and H<sub>2</sub> at different excess air ratio with a temperature of 845 °C and 11 ppm K seeding.

#### 4. Results

The concentration of CO, H<sub>2</sub>, KOH, OH and K for the experimental series listed in Table 2 are shown in Figs. 4–11. The measurements are presented and discussed in two parts corresponding to the two sets of experiments in Table 2: those related to the influence of potassium on CO oxidation at different operating conditions; and those related to the influence of sulfur and chlorine in co-existence with K.

##### 4.1. The effect of operating conditions on inhibition by KOH

Fig. 4 shows results for K atoms and OH measured in a hot flue gas temperature of 845 °C and an excess air ratio of 1.04, i.e. series labelled as K1 in Table 2. The concentration of K atoms increased with the total potassium seeded but levelled out at high potassium loadings. The concentration of OH decreased strongly as the total potassium concentration was increased from 0 to 2 ppm. With potassium levels above 2 ppm, the OH radical concentration in the hot gas was below the detection limit. This shows that the presence of K atoms strongly enhances the consumption of OH radicals in the hot gas environment.

The corresponding concentrations of CO and H<sub>2</sub>, measured by the  $\mu$ -GC, are shown in Fig. 5. The levels of CO and H<sub>2</sub> increased from 0 ppm to 1800 ppm and 700 ppm, respectively, as the potassium seeding increased to 31 ppm. As the concentration of potassium in the flame increases, the concentrations of CO and H<sub>2</sub> increase until they level off. This trend is in agreement with that obtained by Hindiarti et al. [7] in

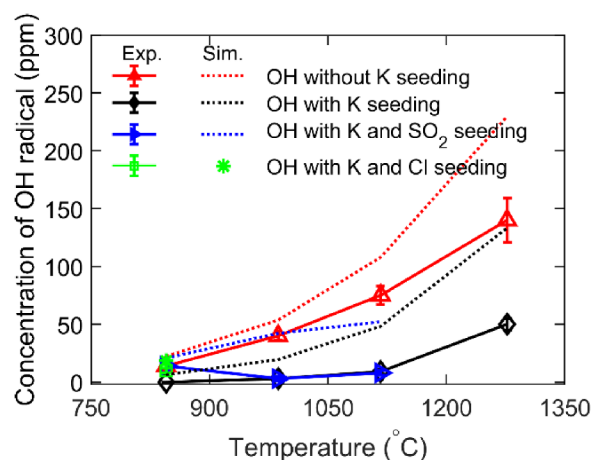


Fig. 9. The variation of the concentration of OH radical at different temperature with an excess air ratio of 1.04. The red line indicates the case without K and SO<sub>2</sub> seeding; black line indicates the case with K seeding but without SO<sub>2</sub> seeding; blue line indicates the case with K and SO<sub>2</sub> seeding. (For interpretation of the references to colour in this figure legend, the reader is referred to the web version of this article.)

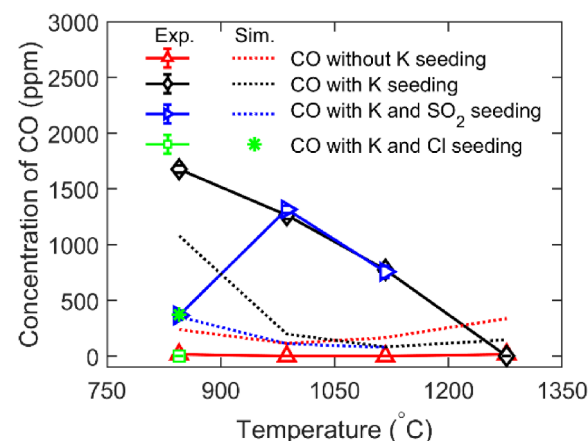


Fig. 10. The variation of the concentration of CO at different temperature with an excess air ratio of 1.04. The red line indicates the case without K and SO<sub>2</sub> seeding; black line indicates the case with K seeding but without SO<sub>2</sub> seeding; blue line indicates the case with K and SO<sub>2</sub> seeding. (For interpretation of the references to colour in this figure legend, the reader is referred to the web version of this article.)

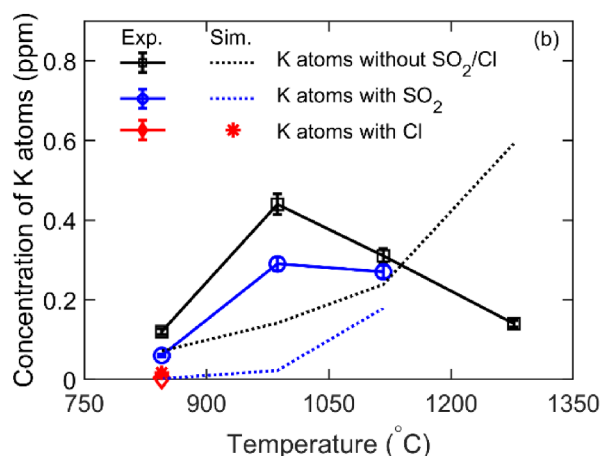
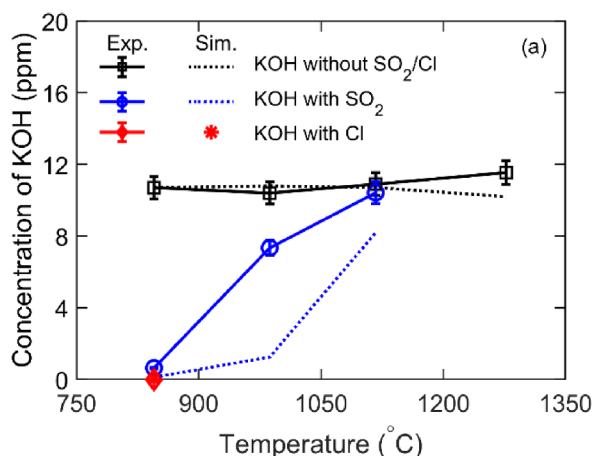


Fig. 8. The variation of the concentration of KOH (a) and K atoms (b) at different temperature and SO<sub>2</sub> seeding at excess air ratio of 1.04 and about 11 ppm of K seeding.

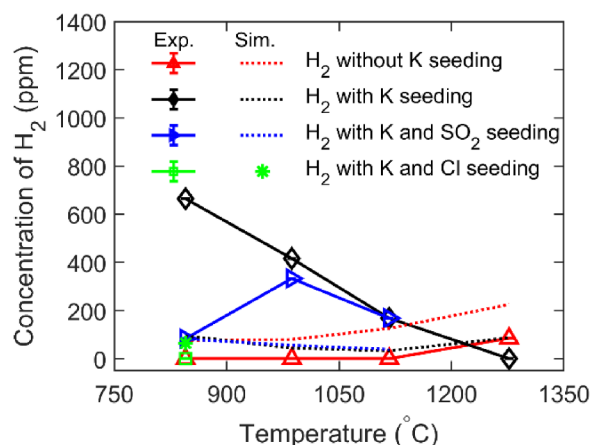


Fig. 11. The variation of the concentration of  $H_2$  at different temperature with an excess air ratio of 1.04. The red line indicates the case without K and  $SO_2$  seeding; black line indicates the case with K seeding but without  $SO_2$  seeding; blue line indicates the case with K and  $SO_2$  seeding. (For interpretation of the references to colour in this figure legend, the reader is referred to the web version of this article.)

moist conditions and in the absence of oxygen. In their case, the concentration of potassium required to saturate the inhibiting effect of potassium was one order of magnitude larger than that obtained in this work in the presence of oxygen. Note that the increase in the levels of unburned CO and  $H_2$  is consistent with the depletion of OH shown in Fig. 4. The results confirm that potassium has a strong inhibiting effect on the oxidation of CO and  $H_2$ .

The modelling predictions are in qualitative agreement with the measurements, but there are quantitative differences. While the K atom concentration is slightly underpredicted, the impact of K on the OH level is significantly smaller than observed. The simulations correctly predict a significant inhibition of the oxidation of CO by the addition of potassium, but the effect on  $H_2$  is underpredicted.

The inhibiting effect of potassium on the oxidation of CO/ $H_2$  in the hot flue gas was also observed at higher excess air ratios, i.e.,  $\lambda = 1.04$ – $1.67$ , as shown in Fig. 6. In this experimental series (series K2 in Table 2), the excess air was adjusted by modifying the amount of air and  $N_2$  in the co-flow. The temperature was kept constant to  $845^\circ\text{C}$  and the potassium seeding to 11 ppm. The concentration of K atoms decreased significantly with the increase of excess air ratio. However, all the cases showed a significant consumption of OH. The concentrations of CO and  $H_2$  are shown in Fig. 7, where the inhibiting effect becomes weaker with the increase of excess air ratio. Under the conditions tested, the inhibiting effect of K on the oxidation of  $H_2$  can no longer be detected at excess air ratios above 1.35.

The simulation results are in reasonable agreement with the experimental data. Similar to the observations at  $\lambda = 1.04$ , the OH concentration in the presence of potassium is overpredicted, while at zero KOH feeding, OH is predicted within 30%.

In the experimental series K3 (see Table 2), the temperature was varied in the range  $845$ – $1275^\circ\text{C}$ , while the excess air ratio was kept at 1.04 and the seeding of  $K_2CO_3$  corresponded to 11 ppm of total potassium. The resulting concentrations of KOH and K atoms are presented in Fig. 8, and the concentration of OH in the cases with and without K is shown in Fig. 9 (see cases without sulfur seeding in the figures). Potassium can enhance the consumption of OH under different temperatures. The corresponding concentrations of CO and  $H_2$  in the hot gas with and without potassium seeding are shown in Fig. 10 and Fig. 11, respectively. The inhibition effect was weakened with the increase of temperature and there is almost no effect as the gas temperature increased to  $1275^\circ\text{C}$ . This is in line with the findings of Ekvall et al. [8] that found no inhibiting effect by potassium at temperatures above  $1000^\circ\text{C}$ .

The model predicts the variation in the concentration of potassium and OH radicals as a function of flue gas temperature satisfactorily. The difference between the trends of the concentration of K atoms obtained in the simulation and in experiment might be caused by the small inhomogeneity of the oxygen concentration in the hot flue gas considering the strong influence of oxygen concentration on the K atom concentration as shown in Fig. 6, but still the simulation and experimental results were at the same concentration level and much smaller than the concentration of KOH as shown in Fig. 8.

#### 4.2. Influence of sulfur and chlorine on K-inhibition

The results derived from the tests with seeding of sulfur are shown in Figs. 8–11, where they are labelled as *with  $SO_2$* . In the cases with co-seeding of potassium (series SK in Table 2), the addition of sulfur show larger influence in the low temperature range compared to the cases at higher temperature. For instance, with the addition of sulfur at  $845^\circ\text{C}$  the concentrations became closer to the conditions without potassium seeding (compare black and blue solid lines in Figs. 10–11). This observation is in line with the sulfation reaction [8]. At  $845^\circ\text{C}$ , the presence of sulfur reduces the formation of K atoms and promotes conversion of KOH to  $K_2SO_4$  particles. Consequently, more OH survived at this temperature, as shown in Fig. 9. Due to the removal of gas phase potassium by the sulfation process the inhibitory effect of potassium is mitigated.

The results prove the interplay between potassium and sulfur in the CO oxidation under the conditions tested, and confirm the hypothesized mechanism involved in the large scale tests at the Chalmers unit [3]. Therefore, the direct effect of sulfur in the oxidation process, as described by several authors for fuels that are free of impurities [11–15] is not sufficient to capture the influence of sulfur in combustion units with more complex fuels. The complexity of the reaction process is increased by the dependence of the behaviour of sulfur at different temperatures as seen in Figs. 10–11 and air excess ratio as described by Alzueta et al. [15].

In the test with seeding of chlorine (CIK in Table 2), the presence of approximately 400 ppm of Cl caused all the potassium in the hot gas to be converted into KCl, which was measured by the UV absorption system, as shown in Fig. 8. After seeding of Cl, a much smaller level of K atoms was detected; about 30 times smaller compared to the KOH case. At the same time, the OH concentration increased from 0 ppm to 10 ppm, as presented in Figs. 8 and 9, while the  $H_2$  and CO concentrations reduced to 0 ppm (cf. Figs. 10 and 11). This is in contrast to the inhibiting effect of Cl on the oxidation of CO commonly reported in literature [17–20], which emphasizes the relevance of the combined effect of active species in complex systems. The data show clearly that the presence of sulphur or chlorine effectively eliminate the inhibition effect of potassium on the CO/ $H_2$ .

The model predicts correctly the removal of KOH and K atoms with  $SO_2$  or Cl seeding, especially at the temperature of  $845^\circ\text{C}$ . Potassium sulfate and potassium chlorine are more stable in the gas phase than potassium hydroxide, resulting in lower predicted concentrations of K atoms in the hot flue gas and higher levels of OH radicals (cf. Fig. 9). As a result, the inhibition effect on CO oxidation is weakened (cf. Fig. 10). However, at the temperature above  $985^\circ\text{C}$ , a larger deviation between the simulation and experimental results was observed.

## 5. Conclusion

This work sheds light on the true mechanism behind insufficient combustion in industrial furnaces in the presence of potassium despite adequate mixing and availability of oxidizer. It is demonstrated that trace level of potassium, i.e. tenths of ppm, inhibits the gas-phase oxidation of CO and  $H_2$  in the temperature range of  $845$ – $1275^\circ\text{C}$  and equivalence ratio of  $1.04$ – $1.65$ . Up to 2000 ppm CO and 700 ppm  $H_2$  was observed to survive the oxidation in oxygen rich hot environments

due to the co-existence of trace amount of potassium. The experiments showed that higher temperature and higher oxygen concentration, respectively, weakens the inhibiting effect of potassium. The reduction of OH concentration due to the existence of K atoms is experimentally measured and identified as the main cause for the inhibition of the oxidation of CO and H<sub>2</sub>. It was further shown that sulfation of the potassium species led the effect to be eliminated. These findings provide an explanation to the casualty between increasing CO concentration and the presence of potassium in flue gases, as well as to the positive impact of sulfur additions in large scale combustion units on the CO emissions. Existing kinetic models capture the qualitative interrelation between potassium, OH radicals, CO and H<sub>2</sub>, respectively, at 845 °C and excess air ratio 1.04, as well as the effect of varying excess air ratio. However, the inhibiting effect of potassium is more intense in practice than what the predictions indicate. The model fails to predict the experimental trends at varying temperature when sulfur and potassium coexist in the combustion environment, and the predictions of H<sub>2</sub> concentration are generally less accurate than those for CO. Overall, this work serves as a basis for the improvement of the theoretical description of the reaction mechanism involved in the inhibition of H<sub>2</sub> and CO oxidation by potassium species and calls for the revision of existing mechanisms.

### Declaration of Competing Interest

The authors declare that they have no known competing financial interests or personal relationships that could have appeared to influence the work reported in this paper.

### Acknowledgements

The research leading to these results received funding from the Swedish Energy Agency (STEM) through the CECOST project and the Swedish gasification centre SFC.

### Appendix A. Supplementary data

Supplementary data to this article can be found online at <https://doi.org/10.1016/j.fuel.2020.117762>.

### References

- [1] M.-o. energidepartementet, Förordning (2013:253) om förbränning av avfall, in: M.-o. energidepartementet (Ed.), 2013.
- [2] Glarborg P. Hidden interactions—trace species governing combustion and emissions. *Proc Combust Inst* 2007;31:77–98.
- [3] Thunman H, Seemann M, Berdugo Vilches T, Maric J, Pallares D, Ström H, et al. Advanced biofuel production via gasification – lessons learned from 200 man-years of research activity with Chalmers' research gasifier and the GoBiGas demonstration plant. *Energy Sci Eng* 2018;6:6–34.
- [4] Marinkovic J, Thunman H, Knutsson P, Seemann M. Characteristics of olive as a bed material in an indirect biomass gasifier. *Chem Eng J* 2015;279:555–66.
- [5] Bulewicz EM, Janicka E, Kandefer S. Halogen inhibition of CO oxidation during the combustion of coal in fluidized bed; 1989. p. 163–8.
- [6] Lissianski VV, Zamansky VM, Maly PM. Effect of metal-containing additives on NO<sub>x</sub> reduction in combustion and reburning. *Combust Flame* 2001;125:1118–27.
- [7] Hindiyarti L, Frandsen F, Livbjerg H, Glarborg P. Influence of potassium chloride on moist CO oxidation under reducing conditions: experimental and kinetic modeling study. *Fuel* 2006;85:978–88.
- [8] Ekvall T, Andersson K. Experimentally observed influences of KCl and SO<sub>2</sub> on CO oxidation in an 80 kW oxy-propane flame. In: International Pittsburgh Coal Conference, Pittsburgh, USA; 2017.
- [9] Friedman R, Levy JB. Inhibition of opposed jet methane-air diffusion flames. The effects of alkali metal vapours and organic halides. *Combust Flame* 1963;7:195–201.
- [10] McHale ET. Flame inhibition by potassium compounds. *Combust Flame* 1975;24:277–9.
- [11] Andersen J. Emission control through sulfur addition. M.Sc. Thesis, Department of Chemical Engineering, Technical University of Denmark, 2006.
- [12] Dam-Johansen K, Amand L-E, Leckner B. Influence of SO<sub>2</sub> on the NON2O chemistry in fluidized bed combustion: 2. Interpretation of full-scale observations based on laboratory experiments. *Fuel* 1993;72:565–71.
- [13] Anthony EJ, Lu Y. Relationship between SO<sub>2</sub> and other pollutant emissions from fluidized-bed combustion. *Symp (Int) Combust* 1998;27:3093–101.
- [14] Miccio F, Löffler G, Wargadalam VJ, Winter F. The influence of SO<sub>2</sub> level and operating conditions on NO<sub>x</sub> and N<sub>2</sub>O emissions during fluidised bed combustion of coals. *Fuel* 2001;80:1555–66.
- [15] Alzueta MU, Bilbao R, Glarborg P. Inhibition and sensitization of fuel oxidation by SO<sub>2</sub>. *Combust Flame* 2001;127:2234–51.
- [16] Weng W, Chen S, Wu H, Glarborg P, Li Z. Optical investigation of gas-phase KCl/KOH sulfation in post flame conditions. *Fuel* 2018;224:461–8.
- [17] Roesler JF, Yetter RA, Dryer FL. The inhibition of the CO/H<sub>2</sub>O<sub>2</sub> reaction by trace quantities of HCl. *Combust Sci Technol* 1992;82:87–100.
- [18] Wu D, Wang Y, Wei X, Li S, Guo X. Experimental investigation and numerical simulation of CO oxidation with HCl addition. *Fuel* 2016;179:221–8.
- [19] Julien S, Brereton CMH, Lim CJ, Grace JR, Anthony EJ. The effect of halides on emissions from circulating fluidized bed combustion of fossil fuels. *Fuel* 1996;75:1655–63.
- [20] Wang J, Anthony EJ. CO oxidation and the inhibition effects of halogen species in fluidised bed combustion. *Combust Theor Model* 2009;13:105–19.
- [21] Weng WB, Borggren J, Li B, Aldén M, Li ZS. A novel multi-jet burner for hot flue gases of wide range of temperatures and compositions for optical diagnostics of solid fuels gasification/combustion. *Rev Sci Instrum* 2017;88.
- [22] Borggren J, Weng WB, Hosseinnia A, Bengtsson PE, Aldén M, Li ZS. Diode laser-based thermometry using two-line atomic fluorescence of indium and gallium. *Appl Phys B-Lasers Opt* 2017;123.
- [23] Gao Q, Weng WB, Li B, Li ZS. Quantitative and spatially resolved measurement of atomic potassium in combustion using diode laser. *Chin Phys Lett* 2018;35.
- [24] Weng W, Brackmann C, Leffler T, Aldén M, Li Z. Ultraviolet absorption cross sections of KOH and KCl for nonintrusive species-specific quantitative detection in hot flue gases. *Anal Chem* 2019;91:4719–26.
- [25] Qu ZC, Steinvall E, Ghorbani R, Schmidt FM. Tunable diode laser atomic absorption spectroscopy for detection of potassium under optically thick conditions. *Anal Chem* 2016;88:3754–60.
- [26] Weng WB, Leffler T, Brackmann C, Aldén M, Li ZS. Spectrally resolved ultraviolet (UV) absorption cross-sections of alkali hydroxides and chlorides measured in hot flue gases. *Appl Spectrosc* 2018;72:1388–95.
- [27] Luque J, Crosley DR. LIFBASE: database and spectral simulation program (Version 1.5). SRI International Report MP 99-009; 1999.
- [28] Luque J, Crosley DR. LIFBASE: database and spectral simulation program (Version 1.5); 1999.
- [29] Design R. CHEMKIN-PRO 15131 San Diego; 2013.
- [30] Weng W, Zhang Y, Wu H, Glarborg P, Li Z. Optical measurement of KOH, KCl and K for quantitative K-Cl chemistry in thermochemical conversion processes, Submitted to Fuel.
- [31] Smith GP, Golden DM, Frenklach M, Moriarty NW, Eiteneer B, Goldenberg M, Bowman CT, Hanson RK, Song S, Gardiner WC, VVJ Jr, Qin Z. GRI-Mech 3.0. [http://www.me.berkeley.edu/gri\\_mech/](http://www.me.berkeley.edu/gri_mech/).
- [32] Glarborg P, Marshall P. Mechanism and modeling of the formation of gaseous alkali sulfates. *Combust Flame* 2005;141:22–39.
- [33] Hindiyarti L, Frandsen F, Livbjerg H, Glarborg P, Marshall P. An exploratory study of alkali sulfate aerosol formation during biomass combustion. *Fuel* 2008;87:1591–600.
- [34] Li B, Sun Z, Li Z, Aldén M, Jakobsen JG, Hansen S, et al. Post-flame gas-phase sulfation of potassium chloride. *Combust Flame* 2013;160:959–69.
- [35] Song Y, Hashemi H, Christensen JM, Zou C, Haynes BS, Marshall P, et al. An exploratory flow reactor study of H<sub>2</sub>S oxidation at 30–100 bar. *Int J Chem Kinet* 2017;49:37–52.
- [36] Pelucchi M, Frassoldati A, Faravelli T, Ruscic B, Glarborg P. High-temperature chemistry of HCl and Cl<sub>2</sub>. *Combust Flame* 2015;162:2693–704.
- [37] Sorvajärvi T, Viljanen J, Toivonen J, Marshall P, Glarborg P. Rate constant and thermochemistry for K + O<sub>2</sub> + N<sub>2</sub> = KO<sub>2</sub> + N<sub>2</sub>. *J Phys Chem A* 2015;119:3329–36.
- [38] Kaskan WE. The reaction of alkali atoms in lean flames. *Symp (Int) Combust* 1965;10:41–6.
- [39] McEwan M, Phillips L. Dissociation energy of NaO<sub>2</sub>. *Trans Faraday Soc* 1966;62.
- [40] Carabetta R, Kaskan WE. Oxidation of sodium, potassium, and cesium in flames. *J Phys Chem* 1968;72:2483–9.
- [41] Hynes AJ, Steinberg M, Schofield K. The chemical kinetics and thermodynamics of sodium species in oxygen-rich hydrogen flames. *J Chem Phys* 1984;80:2585–97.
- [42] Mortensen MR, Hashemi H, Wu H, Glarborg P. Modeling post-flame sulfation of KCl and KOH in bio-dust combustion with full and simplified mechanisms. *Fuel* 2019;258:116147.
- [43] Perry RA, Miller JA. An exploratory investigation of the use of alkali metals in nitrous oxide control. *Int J Chem Kinet* 1996;28:217–34.